ACS APPLIED MATERIALS & INTERFACES

www.acsami.org

Research Article

Sponge-Hosting Polyaniline Array Microstructures for Piezoresistive Sensors with a Wide Detection Range and High Sensitivity

Le Li, Xuran Bao, Jian Meng, Chao Zhang,* and Tianxi Liu*

Cite This: *ACS Appl. Mater. Interfaces* 2022, 14, 30228−30235

Read Online

ACCESS | Metrics & More | Article Recommendations | Supporting Information

ABSTRACT: The development of highly elastic spongy conductors is attractive for use in piezoresistive sensors due to their low cost, easy fabrication, and wide sensing range. However, the combination of high sensitivity and broad sensing range in a single piezoresistive sensor, though highly demanded, is challenging because they are contradictory in principle. Herein, a highly elastic spongy conductor with sponge-hosting polyaniline (PANI) fluff-like array microstructures is fabricated through cryopolymerization. The as-obtained sponge-hosting conductors exhibited an excellent elasticity under high compression strain and stress of up to 80% and 101 kPa, respectively, covering typical deformation ranges for detecting complex human activities. Benefiting from the presence of the sponge-hosting fluff-like PANI arrays, the as-prepared sponge-hosting conductors for piezoresistive sensors possessed a high sensitivity of 0.54 kPa^{-1} in a broad pressure range of 0.1−101 kPa, ascribing to the formation of the sponge-hosting fluff arrays with graded conductive network structures of array contacts and sponge-skeleton contacts at low and high compressions, respectively. As a result, the as-assembled piezoresistive sensors were demonstrated for tactile sensing and human-motion monitoring. This work reveals new approaches for tailored fabrication of sponge-hosting conducting polymers with tunable fluff-like microstructures for highly sensitive and wide-range wearable piezoresistive sensors.

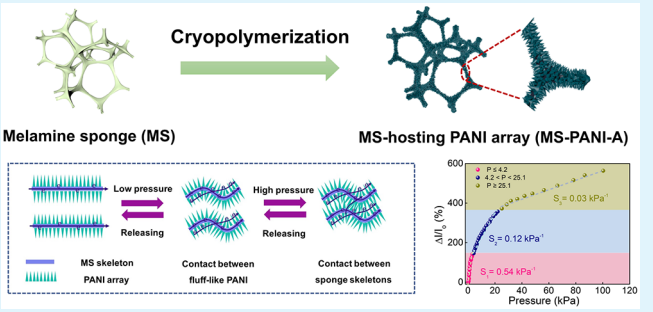

KEYWORDS: *spongy conductor, polyaniline nanoarrays, cryopolymerization, high elasticity, piezoresistive sensor*

INTRODUCTION

Piezoresistive sensors exhibit broad application prospects in wearable electronics because of their simple manufacturing process, easy read-out mechanism, and potential high pixel density.[1−7] The uses of low-intrinsic-modulus elastic matrices are preferred for manufacturing high-performance piezoresistive materials due to their combined advantages of excellent flexibility and high designability.[8−12] One representative example is the use of elastic polymer sponges with a low elastic modulus and high compressive elasticity as elastic matrices that include polyurethane sponges,[13−15] polyimide foams,[16,17] PDMS foams,[18] silane foams,[19] and melamine sponges (MSs).[20−22] Spongy conductors are mainly fabricated by the coating of conductive nanomaterials on the skeleton surface of elastic polymer sponges, and these conductive nanomaterials might include carbon black,[23] graphene,[9,16,18] carbon nanotubes,[24−26] metal nanoparticles,[15] and conducting polymers.[27−29] Responses of electrical signals in spongy conductor-based piezoresistive sensors usually depend on the resistance changes caused by the sponge-skeleton contact.[30] Therefore, piezoresistive sensors based on elastic spongy conductors usually demonstrate undesirable sensitivity, especially in the subtle-pressure region (<1 kPa).

Considerable efforts have been made for improving the sensitivity of piezoresistive sensors in a wide strain range. An effective way to solve this problem is to effectively design the microstructures of elastic conductive materials, and the conductive network could be significantly changed under small pressure, thereby improving the sensitivity of the resultant piezoresistive sensors. In recent years, researchers have demonstrated examples of microstructure engineering to construct high-sensitivity piezoresistive sensors, such as micropyramid arrays,[31] hierarchical structures,[32] interlocked microstructures,[33] porous microstructures,[34] fracture microstructures,[35] and hollow-sphere microstructures.[36] Despite these achievements, the wide application of the above microstructured piezoresistive materials is largely limited by the use of complex manufacturing processes and expensive conductive materials (e.g., graphene, MXene, metal nanoparticles, metal nanowires).[37] Furthermore, the trade-off

Received: April 27, 2022
Accepted: June 7, 2022
Published: June 21, 2022

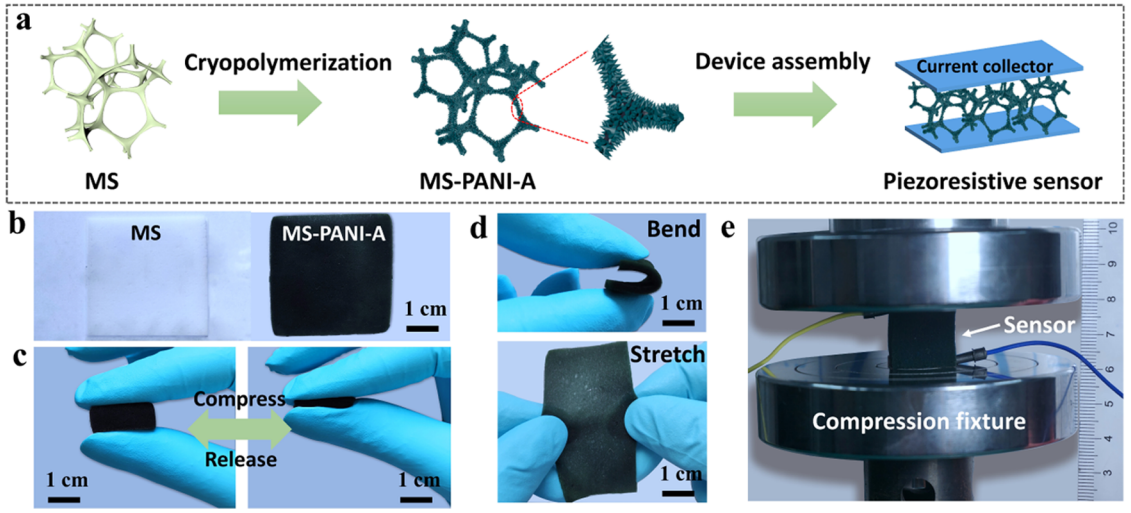

Figure 1. (a) Schematic illustration of the preparation procedure of the MS-PANI-A in piezoresistive sensors. (b) Photograph showing pristine MS and MS-PANI-A. Photographs showing the MS-PANI-A under (c) compressing/releasing processes and (d) bending and stretching processes. (e) Photograph of the MS-PANI-A in piezoresistive sensors.

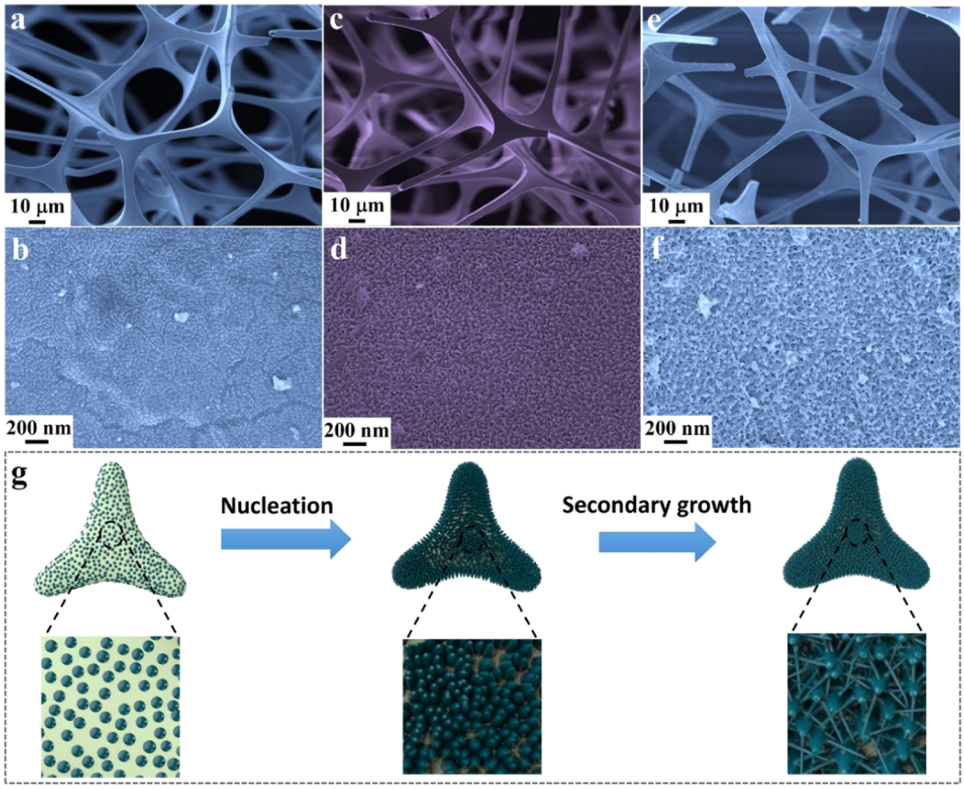

Figure 2. Ex situ morphological observations and formation mechanism for the MS-PANI-A. SEM images of (a, b) MS-PANI-A1, (c, d) MS-PANI-A2, and (e, f) MS-PANI-A3 prepared with cryopolymerization times of 2, 6, and 12 h, respectively. (g) Schematic of the formation mechanism of the MS-PANI-A with the fluff-like array microstructures.

between high sensitivity and a wide sensing range is the key problem of spongy conductor-based piezoresistive sensors because the values of the resistance changes before and after deformation are determined. Therefore, it is of great significance to explore cost-efficient and easy-fabrication strategies for the development of customized spongy conductor-based piezoresistive sensors with high sensitivity and a large working range.

Herein, spongy conductors of melamine sponge-hosting polyaniline (PANI) arrays (MS-PANI-A) are prepared by cryopolymerizion of aniline on commercial elastic sponges, during which the confined nucleation and secondary growth of PANI within the boundaries between ice crystals occurred. The as-grown PANI among the MS-PANI-A demonstrated a fluff-like array morphology on the sponge skeleton of MS. The as-prepared MS-PANI-A could be directly used as piezoresistive materials, which exhibited both a high sensitivity of 0.54 kPa^{-1} and a broad detection range of 0.1−101 kPa. The high sensitivity of the MS-PANI-A piezoresistive sensor is ascribed to the simultaneous formation of graded conductive

https://doi.org/10.1021/acsami.2c07404
ACS Appl. Mater. Interfaces 2022, 14, 30228−30235

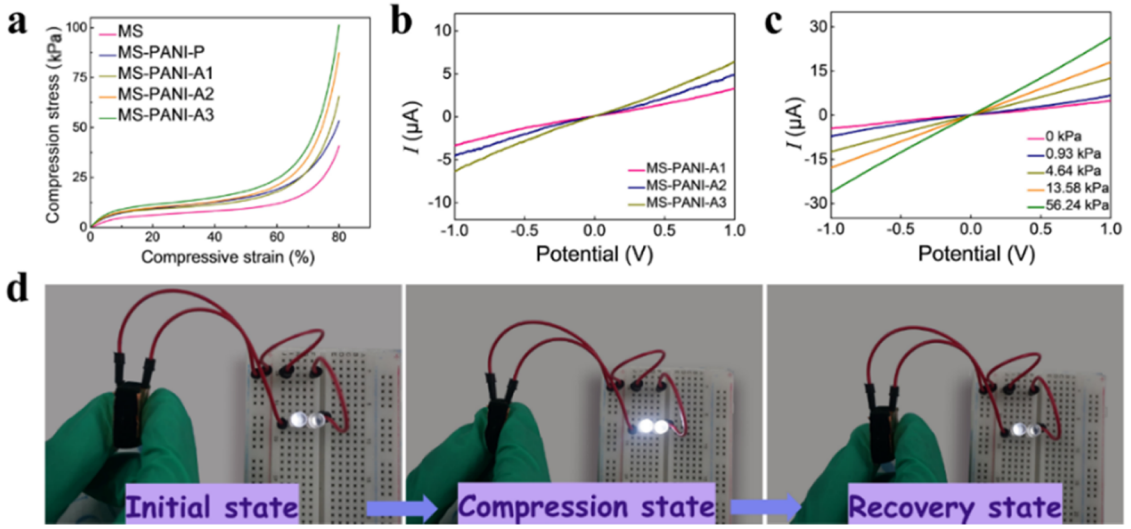

Figure 3. (a) Compressive stress−strain curves of the MS, MS-PANI-P, and MS-PANI-A with an ultimate strain of 80%. (b) *I*−*V* curves of the MS-PANI-A1, MS-PANI-A2, and MS-PANI-A3 without the loading. (c) *I*−*V* curves of the MS-PANI-A2 under various applied pressures. (d) Photographs showing the MS-PANI-A in its initial, compression, and recovery states as a conducting wire in a circuit for illuminating two LED bulbs.

network structures, including the PANI array junction variation and the sponge-skeleton contact−separation under low and high pressures, respectively. The MS-PANI-A piezoresistive sensor also exhibited high elasticity, fast response time, and excellent reproducibility for at least 5000 cycles, demonstrating high potential in wearable sensors for tactile sensing and human-motion monitoring. This study, therefore, provides a simple-yet-efficient route for the fabrication of sponge-hosting conducting polymers for piezoresistive sensors with both high sensitivity and a broad working range.

RESULTS AND DISCUSSION

A schematic of the preparation procedure of MS-PANI-A for piezoresistive sensors is illustrated in Figure 1a. The MS-PANI-A was prepared by the cryopolymerization of aniline using a melamine sponge (MS) as the host. The as-grown PANI exhibited a unique three-dimensional (3D) fluff-like array microstructure during the cryopolymerization process. The MS-PANI-A could well retain the shape and size of pristine MS, while the color changed from white to dark green (Figure 1b). Figure 1c,d shows photographs of the MS-PANI-A when being compressed/released, bent, and stretched, demonstrating its high elasticity for potential use in wearable electronics. Copper wires as current collectors were pasted on the opposite sides of the MS-PANI-A, thus obtaining the corresponding piezoresistive sensor devices (Figure 1e).

Solution-processed polymerization of aniline produced MS-hosting PANI nanoparticles (MS-PANI-P) with a granular morphology of irregular-shaped and aggregated PANI particles (Figure S1), while PANI arrays were easily formed by using the cryopolymerization method (Figure 2). Ex situ scanning electron microscopy (SEM) observations of intermediates at different reaction stages indicated the possible formation mechanism of the PANI arrays with tunable microstructures. At the early stage of cryopolymerization, numerous PANI nucleation centers and growth sites were uniformly distributed on the MS skeletons, which were observed in the MS-PANI-A1 with a cryopolymerization time of 2 h (Figure 2a,b). By further prolonging the cryopolymerization time, these active nucleation centers and growing sites gradually grew into fluff-like arrays (MS-PANI-A2, Figure 2c,d). When the cryopolymerization time was increased to 12 h, 3D porous and interconnected PANI skeletons that were closely wrapped on MS skeletons were observed in the MS-PANI-A3 (Figure 2e,f). Furthermore, the effects of the aniline concentrations and the aniline/ammonium persulfate (APS) molar ratios on the resultant microstructures of MS-PANI-A were also investigated (Figures S2 and S3). Two controlled samples of MS-PANI-A3-1 and MS-PANI-A3-5 with aniline concentrations of 0.01 and 0.05 M, respectively, also exhibited typical morphologies of 3D interconnected PANI skeletons after cryopolymerization for 12 h, which is similar to that of MS-PANI-A3. These results indicate that the influence of the aniline concentrations on the final morphology of MS-PANI-A is negligible (Figure S2). When the aniline/APS molar ratio was changed from 3:1 to 1:1, 3D interconnected and jointed PANI array microstructures were clearly observed in the corresponding samples (Figure S3). This result also indicates that the amounts of oxidants play an important role in the construction of PANI microstructures. The construction of 3D PANI array microstructures could be achieved by suppressing the nucleation reaction and, in the meantime, promoting the secondary growth reaction. Compared to the rough morphology of the MS-PANI-P, the surface engineering for MS-PANI-A through cryopolymerization contributed to the formation of the fluff-like array microstructures of PANI, which is beneficial for increasing the contact areas and sites of conductive components in the spongy conductor, thus providing efficient conductive pathways during compression.

Figure 2g indicates the formation mechanism of PANI arrays induced by cryopolymerization. The growth of PANI arrays experienced the nucleation and growth stages during the cryopolymerization process.[38,39] Initially, the aniline monomer solution was homogeneously adsorbed on the MS hosts due to the hydrogen-bonding interaction between melamine and aniline. Then, the MS with sufficiently adsorbed aniline monomers on the skeleton surface was mixed with oxidants and then quickly frozen. Considering the dilute monomer

https://doi.org/10.1021/acsami.2c07404
ACS Appl. Mater. Interfaces 2022, 14, 30228−30235

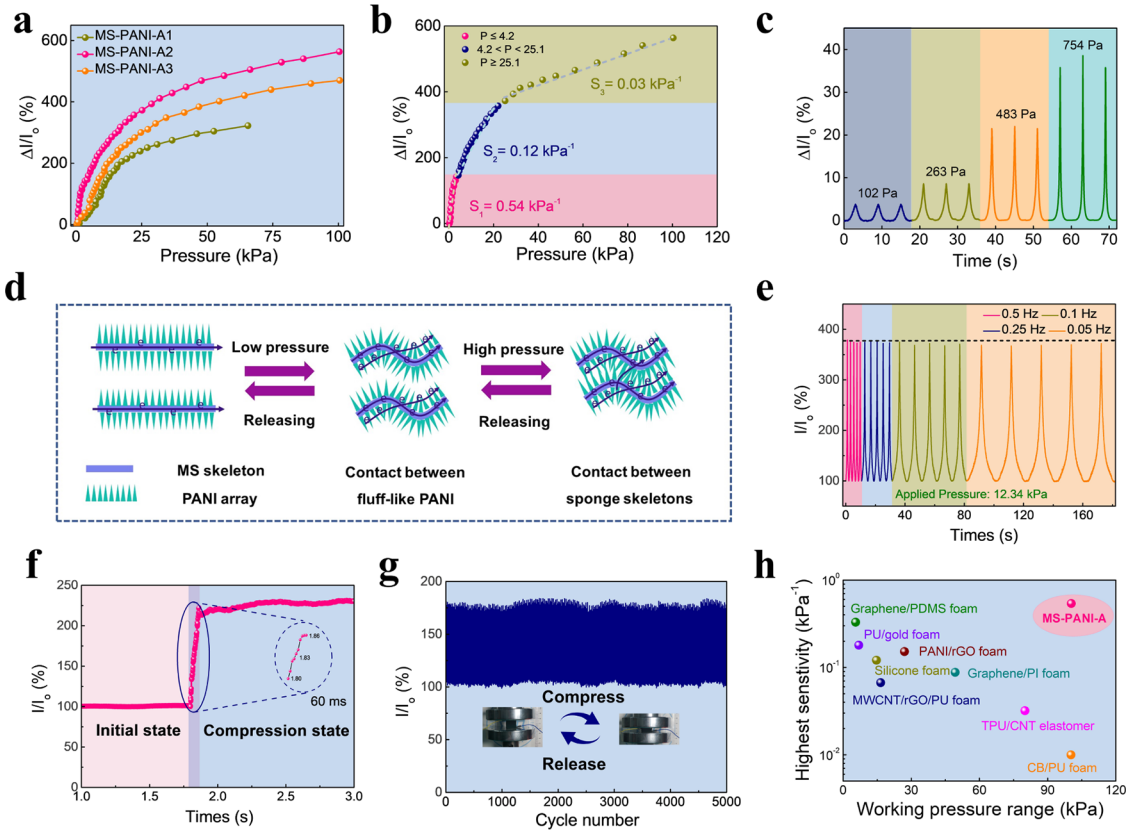

Figure 4. (a) Relative current variations and (b) calculated sensitivity values for the MS-PANI-A sensor. (c) Relative current variations of the MS-PANI-A2 sensor under various ultimate compression stresses. (d) Schematic of the sensing mechanism of the MS-PANI-A under low and high pressures. (e) Frequency-dependent current responses of the MS-PANI-A sensor under the pressure of 12.34 kPa. (f) Response time of the MS-PANI-A2 sensor. (g) Cycling stability of the MS-PANI-A2 sensor under repeated loading/unloading processes at the ultimate pressure of 1 kPa. (h) Comparison of the sensitivity and the ultimate pressure between the MS-PANI-A sensor and other spongy conductor-based piezoresistive sensors in the literature.

concentration and confinement effect of ice crystals, the most active nucleation centers of PANI were formed on MS skeletons. This also minimized the interfacial energy barrier for the subsequent growth of PANI on MS skeletons.[40] The growth stage was largely suppressed due to cryopolymerization under quite low reaction temperature (−30 °C). The slow growth rate is in favor of the growth of PANI along the active nucleation centers generated on MS skeletons; thus, the PANI nanowire arrays were gradually formed within the boundaries between ice crystals in the subsequent secondary growth stage. Finally, the initially formed fluff-like PANI arrays fused to form a 3D porous and interconnected network.

Chemical structures of the PANI array and MS-PANI-A were characterized by Fourier transform infrared (FTIR) spectroscopy (Figure S4). The presence of PANI components within the MS-PANI-A was identified by the presence of typical peaks, including the quinonoid ring vibration at 1491 cm^{-1}, the benzenoid ring vibration at 1572 cm^{-1}, and the C−H stretching vibration on the benzene ring at 790 cm^{-1}.[41] The FTIR peaks at 1283 cm^{-1} (C−N stretching vibration) and 2910 cm^{-1} (C−H stretching vibration) of the MS-PANI-A shifted to relatively high wavenumbers, suggesting the formation of the C−H···N−C hydrogen bonds between the MS substrate and PANI.

The MS, MS-PANI-P, and MS-PANI-A are expected to demonstrate excellent deformation-tolerant performances. Figure 3a exhibits the compressive stress−strain curves of MS, MS-PANI-P, and MS-PANI-A under high compression strains of up to 80%. The compressive stress−strain behaviors of all of these samples exhibited three featured deformation regions, which are always observed in an open-cell sponge structure, namely, an elastic behavior with a linear relationship at the low compression strain (<10%), a typical plateau region due to cell collapse at intermediate compression strain (10−60%), and plastic stiffening at high strain (>60%).[42] The MS exhibited the compressive stress of 40 kPa under an 80% compression strain. After the growth of PANI particles and arrays on sponge skeletons, the resultant MS-PANI-P and MS-PANI-A exhibited largely enhanced compressive stresses of 53 and 101 kPa, respectively. The reinforcement of MS substrates by using the PANI arrays was stronger than the PANI particles, which is ascribed to the formation of sufficient contacting joints for the PANI arrays. These contacting joints could dramatically contribute to efficient energy dissipation, thus enhancing the mechanical strength and toughness of the resultant sponges. The pressure caused by complex human motions can be divided into four pressure regimes: (1) ultralow pressure of <1 Pa (like the sound-caused pressure); (2) subtle pressure from 1 Pa to 1 kPa (like the pulse or heartbeat); (3) low pressure from 1 to 10 kPa (like the daily activity); and (4) medium pressure from 10 to 100 kPa (like the human weight, joint movements).[1] The as-prepared MS-PANI-A with wide compressive strain (0−80%) and stress (0−101 kPa) ranges is able to detect the whole range of human

https://doi.org/10.1021/acsami.2c07404
ACS Appl. Mater. Interfaces 2022, 14, 30228−30235

motions. Figure 3b shows the current−voltage ($I-V$) curves of the MS-PANI-A sensors without any external stimulus. The linear $I-V$ responses of MS-PANI-A indicated its typical ohmic behavior and stable contact between the conductive foam, silver paste, and copper wires. With the increase of the cryopolymerization time, the current output of the MS-PANI-A sensors increased, which is ascribed to the formation of efficient conductive pathways within the MS-PANI-A. The $I-V$ responses of MS-PANI-A sensors under different external pressures are recorded in Figure 3c. The $I-V$ curves indicated that the pressure-sensitive sensing performance of MS-PANI-A was stable under various external pressures. Besides, the corresponding resistance (slope of $I-V$ curves) of MS-PANI-A was constant under each pressure. The integration of elasticity and conductivity in the developed MS-PANI-A indicated its potential for high-performance piezoresistive sensors. A simple electric circuit where the MS-PANI-A is connected to two light-emitting diodes (LEDs) and a power supply is demonstrated in Figure 3d. The LED bulbs could be lighted up by an increased pressure that was applied to the MS-PANI-A sensor with a negative piezoresistive effect, which is attributed to shortened conductive pathways of the spongy conductors during the compression process.

The current response to the pressure of the MS-PANI-A was also evaluated. Figure 4a shows the relative current variations of the MS-PANI-A under a variety of pressures. The relative current variations increased sharply within the low-pressure region (0−25 kPa). The response curves became relatively flat within the high-pressure range, demonstrating the typical piezoresistive behavior.[43] Among these samples, the MS-PANI-A2 sensor with the fluff-like PANI array microstructures demonstrated the optimized sensitivity. In the low-pressure range of 0−4.2 kPa, the sensitivity (S_1) of the MS-PANI-A2 is calculated to be 0.54 kPa^{-1} (Figure 4b), which is higher than the sensitivity of most of the current reported polymer foam-based piezoresistive sensors. As the applied pressure increased progressively, the sensitivity (S_2, S_3) reached 0.12 and 0.03 kPa^{-1} in the pressure region of 4.2−25.1 and 25.1−101 kPa, respectively (Figure 4b). The output current signals of the MS-PANI-A2 sensor under various applied pressures are shown in Figures 4c and S5. The experimental detection limit of the MS-PANI-A2 sensor was found to be 102 Pa (Figure 4c). The output signals of the MS-PANI-A2 sensor maintained almost similar values during loading and unloading processes under a relatively large pressure (Figure S5), proving its excellent reproducibility that is extremely critical for practical application. For comparison, piezoresistive sensors based on the MS-PANI-P with rough PANI nanoparticles on the surface exhibited a relatively low sensitivity, especially in the low-pressure region. The sensitivity of the MS-PANI-P sensor reached only 0.01 kPa^{-1} in the pressure region from 0 to 4.4 kPa (Figure S6). However, the sensitivity of the MS-PANI-A with fluff-like PANI array microstructures was 54 times higher than that of the MS-PANI-P in the low-pressure region. For the MS-PANI-A sensor, the piezoresistive effect is ascribed to the temporary contacts between the sponge-skeleton branches, leading to shortened conductive pathways. However, the contact of sponge-skeleton branches was negligible under small deformation or low pressure, thus resulting in extremely low sensitivity in the low-pressure region. For the MS-PANI-A sensor, the fluff-like PANI arrays evenly distributed on MS skeletons provided sufficient overlapping points to responding external pressure stimulations (Figure 4d). For resistive sensing units, variations of the conductive network structures are the main factors at the initial compression stage.[28] The largely improved sensitivity of the MS-PANI-A2 sensor in the low-pressure region is ascribed to the unique sensing mechanism of PANI array junctions during the deformation. The contact between the adjacent PANI arrays led to shortened conducting pathways under slight compression strain or pressure, which could respond to significant current variations. With the increase of the applied pressures, the sensing mechanism of the sponge-skeleton contact became the dominant factor in determining the sensitivity of the MS-PANI-A2 sensor. The fluff-like PANI array microstructures are beneficial for increasing the contact areas during the compression process, thus providing relatively large conductive variations within sponge skeletons.

The MS-PANI-A2 sensors exhibited stable electrical signals under the applied pressure of 12.34 kPa, as well as stable output signals within the frequency range from 0.05 to 0.5 Hz. These results indicate the reliable frequency-dependent performance of the MS-PANI-A2 sensors under cyclic pressures (Figure 4e). Figure 4f demonstrates the fast response time (<80 ms) of the MS-PANI-A2 sensor during the loading and unloading processes, ensuring real-time sensing responses for monitoring the low-frequency human body signals. Generally, stability under cyclic deformations is the basic requirement for piezoresistive sensors. The stability of the MS-PANI-A2 sensor was investigated by applying a pressure of 1 kPa in long-term cycling tests (Figure 4g). The MS-PANI-A2 sensors exhibited highly stable current responses even after 5000 loading/unloading cycles, which are superior and comparable to other spongy conductors in the literature.[15,17,20,23,25,44−46] Figure S7 shows the current response of the MS-PANI-A2 sensor at the inception, intermediate section, and termination during the cycling tests. The stable current signals indicated that a negligible current deviation occurred during the stability tests. Moreover, the effect of the repeated pressure loadings of the MS-PANI-A2 on its microstructures was investigated by ex situ SEM observations. From the cross-section morphology, close-packed PANI arrays were observed to be wrapped on the MS skeleton without any cracks after 5000 compression/release cycles, proving the high structural integrity of the sensing materials during long-term tests (Figure S8). Furthermore, the drift characteristic of the MS-PANI-A2 sensor was investigated by applying a constant pressure of 3 kPa for 1 h (Figure S9). Here, the "drift characteristics" means the relative changes of output current responses under a certain strain during long periods. For the MS-PANI-A2, only ∼2% drift of the current variations was observed when applying a constant pressure of 3 kPa for 10 h, indicating its capability for long-term applications. The comprehensive performance of the MS-PANI-A2 sensor is comparable to most of the recent spongy conductors in the literature (Figure 4h). The as-fabricated MS-PANI-A sensors possessed an excellent combination of high sensitivity and a wide sensing range, offering advantages of simple synthesis, low cost, and scalable fabrication for piezoresistive materials.

For next-generation sensing devices, functions of tactile sensing and human-activity monitoring are critical to the potential application in human−machine interfaces and e-skin.[47] The potential applications of the MS-PANI-A2 sensor were demonstrated by finger tapping for tactile sensing. To confirm the feasibility of acquiring spatial information, we built a 3 × 3 MS-PANI-A2 sensor array shown in Figure 5a. Figure

https://doi.org/10.1021/acsami.2c07404
ACS Appl. Mater. Interfaces 2022, 14, 30228−30235

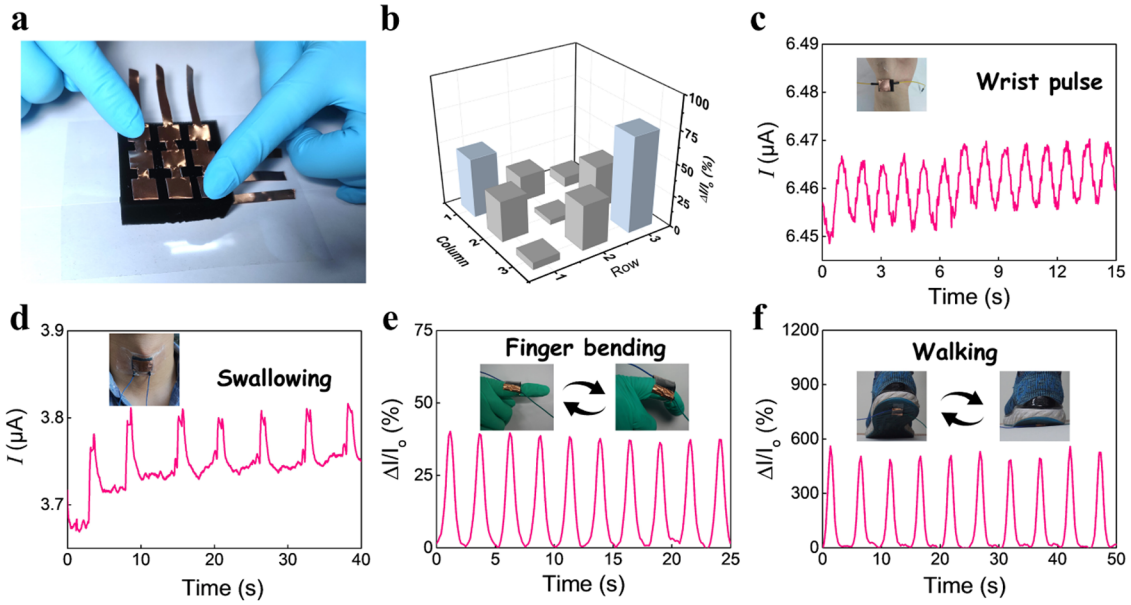

Figure 5. Demonstration of the MS-PANI-A2 sensors for tactile sensing and human-activity monitoring. (a) Photograph of a 3 × 3 sensor array based on individual MS-PANI-A2 sensors. (b) Relative current variations in the sensor array versus pixel location during finger tactile identification. (c) Wrist pulse tactile identification by the MS-PANI-A sensors. The MS-PANI-A2 sensors detecting the motions of (d) swallowing, (e) finger bending, and (f) walking.

5b demonstrates that the MS-PANI-A2 could easily detect and distinguish unique contact points. Besides, the MS-PANI-A2 sensor could monitor the pressures of wrist pulses in real time for disease diagnosis. Figure 5c displays the regular and reproducible signals of wrist pulses when the pressure sensor was fixed onto a wrist. The high-performance sensing performance of the MS-PANI-A2 sensor was investigated for its uses in detecting complex human activities. The fabricated device could be fixed on various locations of the human body like the throat, finger, and foot, indicating the fitness and signal sensing of human body. For real-time monitoring of swallowing, the as-fabricated sensor device was fastened to the throat by adhesive tape and subjected to repeated swallowing processes. Stable output current responses were observed (Figure 5d), demonstrating the linear dependence of the output currents to the applied pressure along with outstanding reproducibility in each successive swallowing process. Subsequently, similar kinds of pressure tests were performed by attaching the sensor to the forefinger and foot. The distinct and stable current responses were recorded during the finger motion and walking process, respectively (Figure 5e,f). These results indicated that the current of the MS-PANI-A2 sensor increased almost linearly with the finger motions and walking. The stable sensing capability of the MS-PANI-A2 for detecting tactile and human activities enables its excellent application in further wearable electronics.

CONCLUSIONS

In summary, we have developed a simple and efficient method to fabricate a superelastic, highly sensitive, and broad-pressure-range sensing platform based on MS-PANI-A with fluff-like PANI array microstructures. The fluff-like PANI arrays with tunable microstructures could be prepared by regulating the nucleation and secondary growth process during the cryopolymerization, which provides a universal and scalable approach to obtain hierarchical conductive networks within spongy conductors without any sophisticated and complex processes. The combination of hierarchical conductive networks including the PANI array junctions and the contact−separation of sponge skeletons endowed the MS-PANI-A piezoresistive sensors with high sensitivity (0.54 kPa^{-1}) and a broad working range (0.1−101 kPa). The MS-PANI-A piezoresistive sensor remarkably exhibited high elasticity withstanding 80% compression strain, fast response time (<80 ms), and good reproducibility (over 5000 cycles). Due to the formation of a versatile pressure sensing platform, various tactile sensing and human activity monitoring, such as wrist pulsing, swallowing, finger bending and walking, could be performed in real time. We believe that this work might provide a unique preparation strategy for microstructure engineering with tunable conducting polymer arrays and inspire new opportunities for the preparation of high-performance spongy conductors with simultaneous high sensitivity and a broad working range.

MATERIALS AND METHODS

Preparation of MS-Hosting PANI Arrays (MS-PANI-A) and MS-Hosting PANI Particles (MS-PANI-P). MS-PANI-A was prepared by the cryopolymerizaion of aniline on MS hosts. A piece of the MS sample was immersed into 30 mL of 0.1 M HCl solution with an aniline concentration of 0.03 M. Another 30 mL of 0.1 M HCl solution containing ammonium persulfate (APS) was added, and the aniline/APS molar ratio was set at 2. The freshly mixed solution was then quickly frozen in liquid nitrogen for 10 min and then left standing at −30 °C for various periods. After being thawed at room temperature, the as-prepared MS-PANI-A was washed with excess water to extract residual reactants and by-products and then dried at 60 °C in a vacuum atmosphere overnight. The as-fabricated MS-PANI-A1, MS-PANI-A2, and MS-PANI-A3 represent the MS-PANI-A samples that were prepared with cryopolymerizaion times of 2, 6, and 12 h, respectively. The comparison sample of MS-PANI-P was prepared by solution-processed polymerization of aniline on MS hosts at 5 °C for 12 h. Furthermore, the MS-PANI-A3-1 and MS-PANI-A3-5 represent the MS-PANI-A3 samples that were prepared by 12-h cryopolymerization with aniline concentrations at 0.01 M and 0.05 M, respectively.

https://doi.org/10.1021/acsami.2c07404
ACS Appl. Mater. Interfaces 2022, 14, 30228−30235

Assembly and Measurements of Piezoresistive Sensors. Two copper wires were connected with the as-fabricated sponge samples (length: 3 cm; width: 2 cm; height: 1 cm) with silver paste to eliminate the contact resistance. The two copper wires were then connected to a digital sourcemeter during compression and release cycles enabled by an Instron universal testing machine. Transparent tapes were utilized to cover the sponge samples to eliminate environmental interferences. The $I-V$ curves of piezoresistive sponges under various pressure loadings were recorded by a Keithley 2601B sourcemeter.

■ ASSOCIATED CONTENT

Supporting Information

The Supporting Information is available free of charge at https://pubs.acs.org/doi/10.1021/acsami.2c07404.

Materials; characterizations; SEM images of MS-PANI-P; SEM images of MS-PANI-A3-1 and MS-PANI-A3-5 after cryopolymerization for 12 h; SEM images of MS-PANI-A prepared with the aniline/APS molar ratio at 3, 2, and 1; FTIR spectra of PANI and MS-PANI-A; current variations of MS-PANI-A2 sensors under pressure applied in steps; relative current variations of MS-PANI-P sensors; current variations of MS-PANI-A2 sensors during cycles; cross-sectional SEM images of MS-PANI-A2 after durability tests; drift characteristics of MS-PANI-A2 sensors under the constant pressure of 3 kPa for 1 h; and the table summarizing the sensing performances of piezoresistive sensors based on the MS-PANI-A and other conducting foams/elastomers in the literature (PDF)

■ AUTHOR INFORMATION

Corresponding Authors

Chao Zhang − *State Key Laboratory for Modification of Chemical Fibers and Polymer Materials, College of Materials Science and Engineering, Donghua University, Shanghai 201620, P. R. China;* orcid.org/0000-0003-1255-7183; Email: czhang@dhu.edu.cn

Tianxi Liu − *Key Laboratory of Synthetic and Biological Colloids, Ministry of Education, School of Chemical and Material Engineering, Jiangnan University, Wuxi 214122, P. R. China;* orcid.org/0000-0002-5592-7386; Email: txliu@jiangnan.edu.cn

Authors

Le Li − *Key Laboratory of Synthetic and Biological Colloids, Ministry of Education, School of Chemical and Material Engineering, Jiangnan University, Wuxi 214122, P. R. China*

Xuran Bao − *Key Laboratory of Synthetic and Biological Colloids, Ministry of Education, School of Chemical and Material Engineering, Jiangnan University, Wuxi 214122, P. R. China*

Jian Meng − *Key Laboratory of Synthetic and Biological Colloids, Ministry of Education, School of Chemical and Material Engineering, Jiangnan University, Wuxi 214122, P. R. China*

Complete contact information is available at: https://pubs.acs.org/10.1021/acsami.2c07404

Author Contributions

The manuscript was written through contributions of all authors. All authors have given approval to the final version of the manuscript.

Notes

The authors declare no competing financial interest.

■ ACKNOWLEDGMENTS

The authors are grateful for the support from the National Natural Science Foundation of China (21875033, 52003107, 52122303), the China Postdoctoral Science Foundation (2021M691266), and the Jiangsu Province Postdoctoral Science Foundation (2021K168B).

■ REFERENCES

(1) Zang, Y.; Zhang, F.; Di, C.-A.; Zhu, D. Advances of Flexible Pressure Sensors toward Artificial Intelligence and Health Care Applications. *Mater. Horiz.* **2015**, *2*, 140−156.

(2) Li, S.; Zhou, X.; Dong, Y.; Li, J. Flexible Self-Repairing Materials for Wearable Sensing Applications: Elastomers and Hydrogels. *Macromol. Rapid Commun.* **2020**, *41*, No. 2000444.

(3) Sun, X.; Yao, F.; Li, J. Nanocomposite Hydrogel-Based Strain and Pressure Sensors: A Review. *J. Mater. Chem. A* **2020**, *8*, 18605−18623.

(4) Guo, Y.; Zhong, M.; Fang, Z.; Wan, P.; Yu, G. A Wearable Transient Pressure Sensor Made with MXene Nanosheets for Sensitive Broad-Range Human-Machine Interfacing. *Nano Lett.* **2019**, *19*, 1143−1150.

(5) Wang, Z.; Cong, Y.; Fu, J. Stretchable and Tough Conductive Hydrogels for Flexible Pressure and Strain Sensors. *J. Mater. Chem. B* **2020**, *8*, 3437−3459.

(6) Huang, Y.; Fan, X.; Chen, S. C.; Zhao, N. Emerging Technologies of Flexible Pressure Sensors: Materials, Modeling, Devices, and Manufacturing. *Adv. Funct. Mater.* **2019**, *29*, No. 1808509.

(7) Li, R.; Tian, X.; Wei, M.; Dong, A.; Pan, X.; He, Y.; Song, X.; Li, H. Flexible Pressure Sensor Based on Cigarette Filter and Highly Conductive MXene Sheets. *Compos. Commun.* **2021**, *27*, No. 100889.

(8) Chen, X.; Liu, H.; Zheng, Y.; Zhai, Y.; Liu, X.; Liu, C.; Mi, L.; Guo, Z.; Shen, C. Highly Compressible and Robust Polyimide/Carbon Nanotube Composite Aerogel for High-Performance Wearable Pressure Sensor. *ACS Appl. Mater. Interfaces* **2019**, *11*, 42594−42606.

(9) Jiang, X.; Ren, Z.; Fu, Y.; Liu, Y.; Zou, R.; Ji, G.; Ning, H.; Li, Y.; Wen, J.; Qi, H. J.; Xu, C.; Fu, S.; Qiu, J.; Hu, N. Highly Compressible and Sensitive Pressure Sensor under Large Strain Based on 3D Porous Reduced Graphene Oxide Fiber Fabrics in Wide Compression Strains. *ACS Appl. Mater. Interfaces* **2019**, *11*, 37051−37059.

(10) Wang, R.; Tan, Z.; Zhong, W.; Liu, K.; Li, M.; Chen, Y.; Wang, W.; Wang, D. Polypyrrole (PPy) Attached on Porous Conductive Sponge Derived from Carbonized Graphene Oxide Coated Polyurethane (PU) and Its Application in Pressure Sensor. *Compos. Commun.* **2020**, *22*, No. 100426.

(11) Luo, M.; Li, M.; Li, Y.; Chang, K.; Liu, K.; Liu, Q.; Wang, Y.; Lu, Z.; Liu, X.; Wang, D. In-Situ Polymerization of PPy/Cellulose Composite Sponge with High Elasticity and Conductivity for the Application of Pressure Sensor. *Compos. Commun.* **2017**, *6*, 68−72.

(12) Fan, C.; Wang, D.; Huang, J.; Ke, H.; Wei, Q. A Highly Sensitive Epidermal Sensor Based on Triple-Bonded Hydrogels for Strain/Pressure Sensing. *Compos. Commun.* **2021**, *28*, No. 100951.

(13) Liu, H.; Dong, M. Y.; Huang, W. J.; Gao, J. C.; Dai, K.; Guo, J.; Zheng, G. Q.; Liu, C. T.; Shen, C. Y.; Guo, Z. H. Lightweight Conductive Graphene/Thermoplastic Polyurethane Foams with Ultrahigh Compressibility for Piezoresistive Sensing. *J. Mater. Chem. C* **2017**, *5*, 73−83.

(14) Ma, Z.; Wei, A.; Ma, J.; Shao, L.; Jiang, H.; Dong, D.; Ji, Z.; Wang, Q.; Kang, S. Lightweight, Compressible and Electrically Conductive Polyurethane Sponges Coated with Synergistic Multi-walled Carbon Nanotubes and Graphene for Piezoresistive Sensors. *Nanoscale* **2018**, *10*, 7116−7126.

(15) Wu, Y. H.; Liu, H. Z.; Chen, S.; Dong, X. C.; Wang, P. P.; Liu, S. Q.; Lin, Y.; Wei, Y.; Liu, L. Channel Crack-Designed Gold@PU

Sponge for Highly Elastic Piezoresistive Sensor with Excellent Detectability. *ACS Appl. Mater. Interfaces* **2017**, *9*, 20098−20105.
(16) Huang, J.; Wang, J.; Yang, Z.; Yang, S. High-Performance Graphene Sponges Reinforced with Polyimide for Room-Temperature Piezoresistive Sensing. *ACS Appl. Mater. Interfaces* **2018**, *10*, 8180−8189.
(17) Qin, Y.; Peng, Q.; Ding, Y.; Lin, Z.; Wang, C.; Li, Y.; Xu, F.; Li, J.; Yuan, Y.; He, X.; Li, Y. Lightweight, Superelastic, and Mechanically Flexible Graphene/Polyimide Nanocomposite Foam for Strain Sensor Application. *ACS Nano* **2015**, *9*, 8933−8941.
(18) Pang, Y.; Tian, H.; Tao, L.; Li, Y.; Wang, X.; Deng, N.; Yang, Y.; Ren, T. L. Flexible, Highly Sensitive, and Wearable Pressure and Strain Sensors with Graphene Porous Network Structure. *ACS Appl. Mater. Interfaces* **2016**, *8*, 26458−26462.
(19) Yu, X. G.; Li, Y. Q.; Zhu, W. B.; Huang, P.; Wang, T. T.; Hu, N.; Fu, S. Y. A Wearable Strain Sensor Based on a Carbonized Nano-Sponge/Silicone Composite for Human Motion Detection. *Nanoscale* **2017**, *9*, 6680−6685.
(20) Ge, G.; Cai, Y.; Dong, Q.; Zhang, Y.; Shao, J.; Huang, W.; Dong, X. A Flexible Pressure Sensor Based on rGO/Polyaniline Wrapped Sponge with Tunable Sensitivity for Human Motion Detection. *Nanoscale* **2018**, *10*, 10033−10040.
(21) Liu, Z.; Wan, K.; Zhu, T.; Zhu, J.; Xu, J.; Zhang, C.; Liu, T. X. Superelastic, Fatigue-Resistant, and Flame-Retardant Spongy Conductor for Human Motion Detection against a Harsh High-Temperature Condition. *ACS Appl. Mater. Interfaces* **2021**, *13*, 7580−7591.
(22) Ding, Y.; Yang, J.; Tolle, C. R.; Zhu, Z. Flexible and Compressible PEDOT:PSS@Melamine Conductive Sponge Prepared Via One-Step Dip Coating as Piezoresistive Pressure Sensor for Human Motion Detection. *ACS Appl. Mater. Interfaces* **2018**, *10*, 16077−16086.
(23) Wu, X.; Han, Y.; Zhang, X.; Zhou, Z.; Lu, C. Large Area Compliant, Low Cost, and Versatile Pressure Sensing Platform Based on Microcrack Designed Carbon Black@Polyurethane Sponge for Human-Machine Interfacing. *Adv. Funct. Mater.* **2016**, *26*, 6246.
(24) Iglio, R.; Mariani, S.; Robbiano, V.; Strambini, L.; Barillaro, G. Flexible Polydimethylsiloxane Foams Decorated with Multiwalled Carbon Nanotubes Enable Unprecedented Detection of Ultralow Strain and Pressure Coupled with a Large Working Range. *ACS Appl. Mater. Interfaces* **2018**, *10*, 13877−13885.
(25) Tewari, A.; Gandla, S.; Bohm, S.; McNeill, C. R.; Gupta, D. Highly Exfoliated Mwnt-Rgo Ink-Wrapped Polyurethane Foam for Piezoresistive Pressure Sensor Applications. *ACS Appl. Mater. Interfaces* **2018**, *10*, 5185−5195.
(26) Lin, M.; Zheng, Z.; Yang, L.; Luo, M.; Fu, L.; Lin, B.; Xu, C. A High-Performance, Sensitive, Wearable Multifunctional Sensor Based on Rubber/CNT for Human Motion and Skin Temperature Detection. *Adv. Mater.* **2021**, *34*, No. 2107309.
(27) Wang, C.; Ding, Y.; Yuan, Y.; Cao, A.; He, X.; Peng, Q.; Li, Y. Multifunctional, Highly Flexible, Free-Standing 3D Polypyrrole Foam. *Small* **2016**, *12*, 4070−4076.
(28) Wang, P.; Wang, M.; Zhu, J.; Wang, Y.; Gao, J.; Gao, C.; Gao, Q. Surface Engineering Via Self-Assembly on PEDOT: PSS Fibers: Biomimetic Fluff-Like Morphology and Sensing Application. *Chem. Eng. J.* **2021**, *425*, No. 131551.
(29) Zheng, S.; Wu, X.; Huang, Y.; Xu, Z.; Yang, W.; Liu, Z.; Huang, S.; Xie, B.; Yang, M. Highly Sensitive and Multifunctional Piezoresistive Sensor Based on Polyaniline Foam for Wearable Human-Activity Monitoring. *Composites, Part A* **2019**, *121*, 510−516.
(30) Liu, Z.; Li, G.; Qin, Q.; Mi, L.; Li, G.; Zheng, G.; Liu, C.; Li, Q.; Liu, X. Electrospun PVDF/PAN Membrane for Pressure Sensor and Sodium-Ion Battery Separator. *Adv. Compos. Hybrid Mater.* **2021**, *4*, 1215−1225.
(31) Choong, C. L.; Shim, M. B.; Lee, B. S.; Jeon, S.; Ko, D. S.; Kang, T. H.; Bae, J.; Lee, S. H.; Byun, K. E.; Im, J.; Jeong, Y. J.; Park, C. E.; Park, J. J.; Chung, U. I. Highly Stretchable Resistive Pressure Sensors Using a Conductive Elastomeric Composite on a Micropyramid Array. *Adv. Mater.* **2014**, *26*, 3451−3458.
(32) Jia, J.; Pu, J.-H.; Liu, J.-H.; Zhao, X.; Ke, K.; Bao, R.-Y.; Liu, Z.-Y.; Yang, M.-B.; Yang, W. Surface Structure Engineering for a Bionic Fiber-Based Sensor toward Linear, Tunable, and Multifunctional Sensing. *Mater. Horiz.* **2020**, *7*, 2450−2459.
(33) Pang, C.; Lee, G. Y.; Kim, T. I.; Kim, S. M.; Kim, H. N.; Ahn, S. H.; Suh, K. Y. A Flexible and Highly Sensitive Strain-Gauge Sensor Using Reversible Interlocking of Nanofibres. *Nat. Mater.* **2012**, *11*, 795−801.
(34) Jung, S.; Kim, J. H.; Kim, J.; Choi, S.; Lee, J.; Park, I.; Hyeon, T.; Kim, D.-H. Reverse-Micelle-Induced Porous Pressure-Sensitive Rubber for Wearable Human-Machine Interfaces. *Adv. Mater.* **2014**, *26*, 4825−4830.
(35) Yao, H. B.; Ge, J.; Wang, C. F.; Wang, X.; Hu, W.; Zheng, Z. J.; Ni, Y.; Yu, S. H. A Flexible and Highly Pressure-Sensitive Graphene-Polyurethane Sponge Based on Fractured Microstructure Design. *Adv. Mater.* **2013**, *25*, 6692−6698.
(36) Pan, L.; Chortos, A.; Yu, G.; Wang, Y.; Isaacson, S.; Allen, R.; Shi, Y.; Dauskardt, R.; Bao, Z. An Ultra-Sensitive Resistive Pressure Sensor Based on Hollow-Sphere Microstructure Induced Elasticity in Conducting Polymer Film. *Nat. Commun.* **2014**, *5*, No. 3002.
(37) Xie, W.; Yao, F.; Gu, H.; Du, A.; Lei, Q.; Naik, N.; Guo, Z. Magnetoresistive and Piezoresistive Polyaniline Nanoarrays in-Situ Polymerized Surrounding Magnetic Graphene Aerogel. *Adv. Compos. Hybrid Mater.* **2022**, DOI: 10.1007/s42114-021-00413-y.
(38) Wang, K.; Wu, H.; Meng, Y.; Wei, Z. Conducting Polymer Nanowire Arrays for High Performance Supercapacitors. *Small* **2014**, *10*, 14−31.
(39) Tran, H. D.; Wang, Y.; D'Arcy, J. M.; Kaner, R. B. Toward an Understanding of the Formation of Conducting Polymer Nanofibers. *ACS Nano* **2008**, *2*, 1841−1848.
(40) Chiou, N. R.; Lu, C.; Guan, J.; Lee, L. J.; Epstein, A. J. Growth and Alignment of Polyaniline Nanofibres with Superhydrophobic, Superhydrophilic and Other Properties. *Nat. Nanotechnol.* **2007**, *2*, 354−357.
(41) Li, L.; Zhang, Y.; Lu, H.; Wang, Y.; Xu, J.; Zhu, J.; Zhang, C.; Liu, T. X. Cryopolymerization Enables Anisotropic Polyaniline Hybrid Hydrogels with Superelasticity and Highly Deformation-Tolerant Electrochemical Energy Storage. *Nat. Commun.* **2020**, *11*, No. 62.
(42) Li, L.; Wang, K.; Huang, Z. Q.; Zhang, C.; Liu, T. X. Highly Ordered Graphene Architectures by Duplicating Melamine Sponges as a Three-Dimensional Deformation-Tolerant Electrode. *Nano Res.* **2016**, *9*, 2938−2949.
(43) Wu, P.; Xiao, A.; Zhao, Y.; Chen, F.; Ke, M.; Zhang, Q.; Zhang, J.; Shi, X.; He, X.; Chen, Y. An Implantable and Versatile Piezoresistive Sensor for the Monitoring of Human-Machine Interface Interactions and the Dynamical Process of Nerve Repair. *Nanoscale* **2019**, *11*, 21103−21118.
(44) Atalay, O.; Atalay, A.; Gafford, J.; Walsh, C. A Highly Sensitive Capacitive-Based Soft Pressure Sensor Based on a Conductive Fabric and a Microporous Dielectric Layer. *Adv. Mater. Technol.* **2018**, *3*, No. 1700237.
(45) He, Z.; Chen, W.; Liang, B.; Liu, C.; Yang, L.; Lu, D.; Mo, Z.; Zhu, H.; Tang, Z.; Gui, X. Capacitive Pressure Sensor with High Sensitivity and Fast Response to Dynamic Interaction Based on Graphene and Porous Nylon Networks. *ACS Appl. Mater. Interfaces* **2018**, *10*, 12816−12823.
(46) Lee, J.; Kim, J.; Shin, Y.; Jung, I. Ultra-Robust Wide-Range Pressure Sensor with Fast Response Based on Polyurethane Foam Doubly Coated with Conformal Silicone Rubber and CNT/TPU Nanocomposites Islands. *Composites, Part B* **2019**, *177*, No. 107364.
(47) Chhetry, A.; Sharma, S.; Yoon, H.; Ko, S.; Park, J. Y. Enhanced Sensitivity of Capacitive Pressure and Strain Sensor Based on $CaCu_3Ti_4O_{12}$ Wrapped Hybrid Sponge for Wearable Applications. *Adv. Funct. Mater.* **2020**, *30*, No. 1910020.